Ordered phases of potassium on Pt{111}: Experiment and theory

S. Moré, W. Berndt, and A. M. Bradshaw
Fritz-Haber-Institut der Max-Planck-Gesellschaft, Faradayweg 4-6, D-14195 Berlin, Germany

Roland Stumpf
Sandia National Laboratories, Albuquerque, New Mexico 87185-1413

(Received 23 September 1997)

Using low-energy electron diffraction structural analysis and first-principles calculations based on the local-density approximation we have investigated the $(\sqrt{3}\times\sqrt{3})R30°$ K and (2×2) K overlayers on Pt{111}. The measured and calculated adsorption geometries agree quantitatively. In both phases the K adatoms occupy threefold symmetric hcp hollow sites, the preference for the hcp site over the fcc site being a consequence of the polarization of the surface Pt *d* electrons. We have not found any indication of K incorporation into the Pt{111} surface, as has been recently suggested. [S0163-1829(98)06412-1]

I. INTRODUCTION

CO and potassium on Pt{111} represents an important model system in studies of alkali metal coadsorption. Indeed, the first measurements showing the typical features of the interaction between the two species were first performed for this system some fifteen years ago.[1,2] Both the pure layers of each adsorbate and the co-adsorbed layer give rise to ordered phases. A necessary prerequisite for understanding the nature of the interaction, and the promotion effects of alkali metals in catalytic reactions involving CO, is a knowledge of the structure of these phases. In this paper we concentrate on two ordered phases in the pure K layer. Altogether five are known: At low coverage a (3×3) structure is first formed followed by the $(\sqrt{7}\times\sqrt{7})R19°$, (2×2) $(\sqrt{3}\times\sqrt{3})R30°$, and $(3/2\times3/2)$ phases.[1,3] This series can be interpreted as resulting from a minimization of the electrostatic K-K repulsion,[4] which according to the widely accepted Gurney model is caused by a transfer of charge to the Pt surface and the resulting interaction between the partially charged K adatoms. In agreement with this model, a threefold symmetric adsorption site at low coverage has been predicted by cluster calculations within the LDA by Müller.[5,6] Based on measurements with various (semiquantitative) techniques Lehmann, Ross, and Bertel[7] have suggested, however, that K (and Na) incorporate partially into the Pt{111} surface below a coverage of $\Theta=0.22$ without a measurable activation barrier. (The coverage $\Theta=0.33$ corresponds to the $(\sqrt{3}\times\sqrt{3})R30°$ phase with one adatom per unit cell.) On the basis of electron-energy-loss spectroscopy (EELS) and scanning tunneling microscopy (STM) Hannon *et al.*[6] have also suggested that substitutional adsorption occurs. They found that the incorporation is an activated process that only takes place at a K coverage $\Theta=0.1$ or higher. This adsorption site would mean that Pt-Pt bonds would have to be broken in favor of Pt-K bonds.

We present a dynamical LEED structural analysis of K adsorbed on Pt{111} in the (2×2) and $(\sqrt{3}\times\sqrt{3})R30°$ phases at coverages of $\Theta=0.25$ and $\Theta=0.33$, respectively, at 100 K. These are compared to our LDA-based first-principles calculations, which give very similar surface geometries. Both indicate that the hcp site is the stable site for K on the Pt{111} surface, although there is only a very small energy difference (15 meV) between the two threefold symmetric hollow sites. In order to study the energetics of possible K incorporation we have also calculated the stability of several intermixed phases at high K coverage, but do not find an energetically favorable substitutional geometry.

II. SAMPLE PREPARATION AND LEED MEASUREMENT

A 5N Pt crystal of dimensions $8\times8\times2$ mm was oriented to within 0.5 degrees of the {111} orientation. The temperature was measured using a Ni/NiCr thermocouple and it could be varied through resistive heating between 90 K and 1400 K using a programmable power control unit. To clean the surface several cycles of argon ion bombardment and subsequent annealing to 800 K were required. Auger measurements show that carbon was the main contaminant. Using the cleaning cycle contamination could be reduced until the ratio between the Auger amplitudes from carbon at 272 eV and platinum at 64 eV was 4×10^{-4}. K was deposited from a commercial SAES getter source [SAES Getters SpA] with the crystal held at 100 K. The source was thoroughly out-gassed prior to each experiment. For a constant evaporation rate the amount of K on the Pt{111} surface, as measured by the Auger signal, was found to increase linearly with time, indicating a two-dimensional growth of the overlayer. Both the $(\sqrt{3}\times\sqrt{3})R30°$ and the (2×2) structures were found to be stable for at least 1 h at 100 K. Adsorption at room temperature or adsorption at 100 K and subsequent annealing at 270 K did not change the measured $I(V)$ curves substantially. All experiments were carried out at background pressures below 10^{-10} mbar.

The LEED intensities at 100 K sample temperature were measured using a Varian three-grid optics and a video-LEED system (AIDA) from Vacuum Science Instruments. The LEED patterns from the clean surface as well as from the overlayer structures were characterized by sharp spots and a low background intensity. The energy of the electron beam was varied in steps of 1 eV from 40–50 eV to 400 eV. Five, thirteen, and nine $I(V)$ curves were taken for the clean surface, the (2×2) K overlayer (Fig. 1), and the $(\sqrt{3}\times\sqrt{3})R30°$ K overlayer (Fig. 2) and, respectively, com-

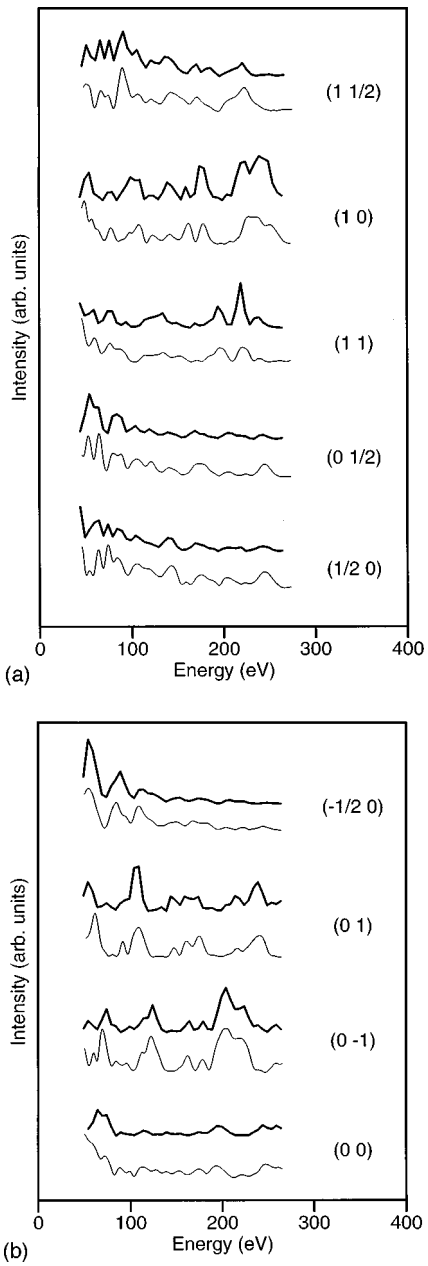

FIG. 1. Experimental (thin lines) and calculated best-fit $I(V)$ curves (thick lines) obtained from Pt{111}(2×2)-K at 100 K. (a) normal incidence, (b) off-normal incidence.

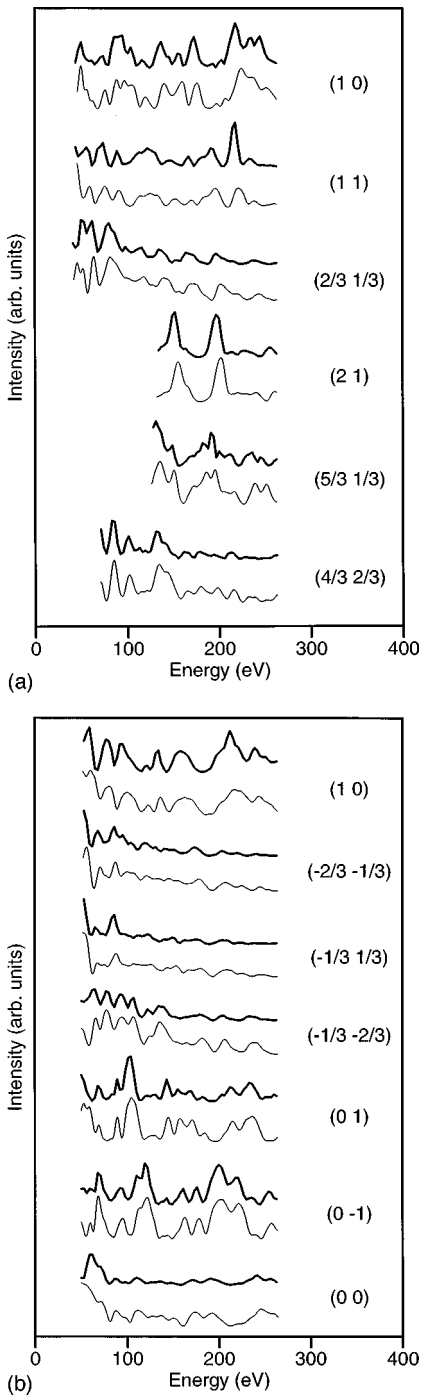

FIG. 2. Experimental (thin lines) and calculated best-fit $I(V)$ curves (thick lines) obtained from Pt{111}$(\sqrt{3}\times\sqrt{3})R30°$-K at 100 K. (a) normal incidence, (b) off-normal incidence.

pared to dynamical LEED calculations.

III. THE LEED-*IV* ANALYSIS

The LEED results were analyzed using a fully dynamical multiple scattering code developed by Moritz.[8] The program uses the layer KKR and the ''layer-doubling'' method.[9] For the Pt atomic potential phase shifts up to $l=11$ derived from self-consistent band-structure calculations were used. For K the potential from Ref. 10 was used. To determine the adsorption structure a grid search involving the adsorbate position and the first two-layer distances was performed. The agreement between the calculated and measured $I(V)$ curves was quantified by the R_P (Ref. 11) and R_{DE} (Ref. 12) reliability factors. The following high-symmetry geometries were considered in the analysis [Fig. 3 shows them for the (2×2) structures]: the threefold-hollow sites (hcp and fcc), the bridge site, and the atop site. Additionally, we tried a surface substitutional geometry similar to the one proposed for Na and K on Al(111) (Ref. 13) [Fig. 3(e)] and a structure with $\Theta=1/9$ subsurface K and with $\Theta=2/9$ K on the surface in hcp sites [Fig. 3(f)].

A hollow site geometry clearly resulted in the smallest R factors. Both the hcp and fcc geometries for the (2×2) phase were further refined, based on minimizing R_P, by considering a rumpling of the first substrate layer with two in-

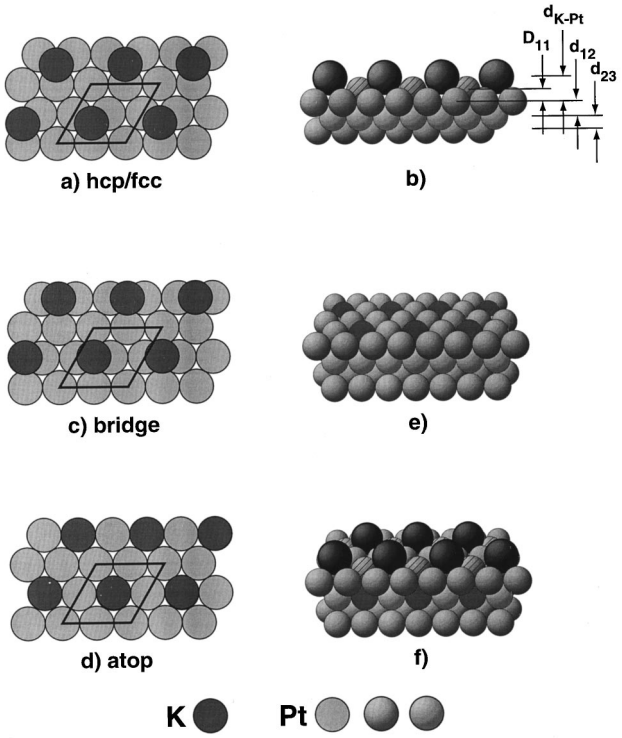

FIG. 3. Models for the (2×2) phase investigated in the LEED $I(V)$ analysis.

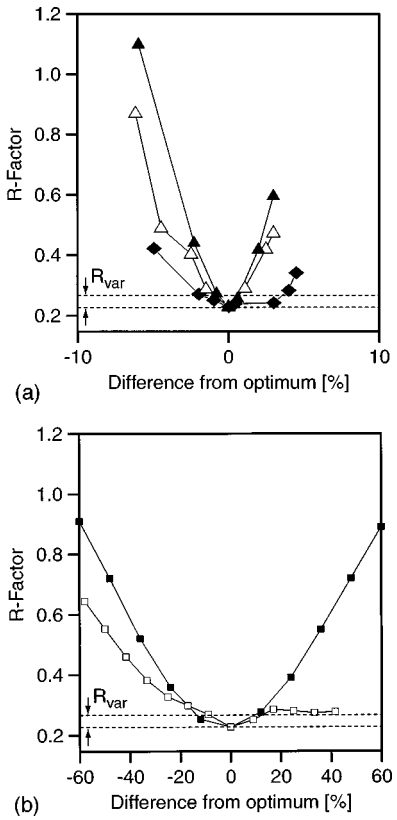

FIG. 4. R factor minima for various structural and nonstructural parameters for Pt{111}$(\sqrt{3}\times\sqrt{3})R30°$-K. The region between the dashed lines (R_{var}) indicates the variance interval as estimated from the formula of Pendry (Ref. 12). (a) △ (filled), separation between K and first Pt layer $d_{K\text{-}Pt}$; △, separation between first and second Pt layer d_{12}; ◇ (filled), separation between second and third Pt layer d_{12}. (b) □ (filled), real part of the complex inner potential V_0; □, split-position distance in [Å].

equivalent Pt surface atoms [see Fig. 3(b)]. We subsequently optimized the Debye temperatures and simulated the vibrational motion of the K atoms for both phases by using the method of split positions.[14] Plots of the R factor for the $(\sqrt{3}\times\sqrt{3})R30°$ structure against the various structural parameters are shown in Fig. 4.

IV. GEOMETRY FROM THE LEED ANALYSIS

A. The clean Pt{111} surface

The best fit between experiment and simulations is obtained for a first-layer expansion of $\Delta d_{12}=1.5\pm0.9\%$ ($d_{12}=2.30\pm0.02$ Å). The spacing between deeper layers is indistinguishable from the bulk value. The Pendry R factor is 0.24 for normal incidence and 0.28 for off-normal incidence. The inner potential was chosen to be -7.5 eV with an imaginary part $V_{0i}=V_{0ic}[(E-V_{0r})/eV]^{1/3}$. The constant V_{0ic} minimizes R_P at $V_{0i}=0.75$ eV. The results fall within the error margins of earlier experimental results.[12,15]

B. Adsorbate structures

In the ''best fit'' structure [Fig. 5(a)] for the (2×2) phase the K atoms are located in the hcp hollow site, with a bond length of 3.12 ± 0.04 Å between the K and the three nearest-neighbor platinum surface atoms. The Pt surface atoms that are nearest neighbors of the K adsorbates are raised relative to the other Pt surface atoms by 0.07 Å(D_{11}). The average first interlayer spacing is expanded by 1%. No expansion or contraction is measurable for deeper layers. In the optimized $(\sqrt{3}\times\sqrt{3})R30°$ structure [Fig. 5(a)] the K atoms are also adsorbed in hcp hollow sites with a bond length of 3.15 ±0.02 Å between the K and platinum atoms in the first layer. The platinum atom in the second layer below is at a distance of 5.01 Å. The first layer spacing is expanded by 1.0%, the second-layer distance is contracted by 0.5% relative to the bulk layer distance.

(2×2) and $(\sqrt{3}\times\sqrt{3})R30°$ phases of alkali metals on threefold-symmetric hollow sites have been observed for K, Rb, and Cs on Rh{111}, Ru{0001}, and Ag{111}.[16–18] A small rumpling of the first substrate layer for the (2×2) phases has also been observed earlier.[17] There is, however, one significant difference in the Pt case. For both Ru{0001} and Ag{111} the alkali adsorption site changes from the fcc site at low coverage to the hcp site at high coverage. This is not the case for K on Pt{111}. A change from the fcc site to the hcp site with increasing coverage could be safely excluded in our LEED analysis (See Table I and Figs. 1 and 4). We discuss the origin of this preference for the hcp site in Sec. VI E below.

The LEED analysis also excludes the possibility of a significant fraction of substitutional or subsurface K adsorption geometries. This is not in direct contradiction to reports of K being incorporated into the Pt{111} surface by Hannon *et al.*[6] because all our experiments were conducted below 270 K and at a higher coverage. According to this reference the incorporation required heating the sample to room temperature following a significant length of time. Lehmann, Ross,

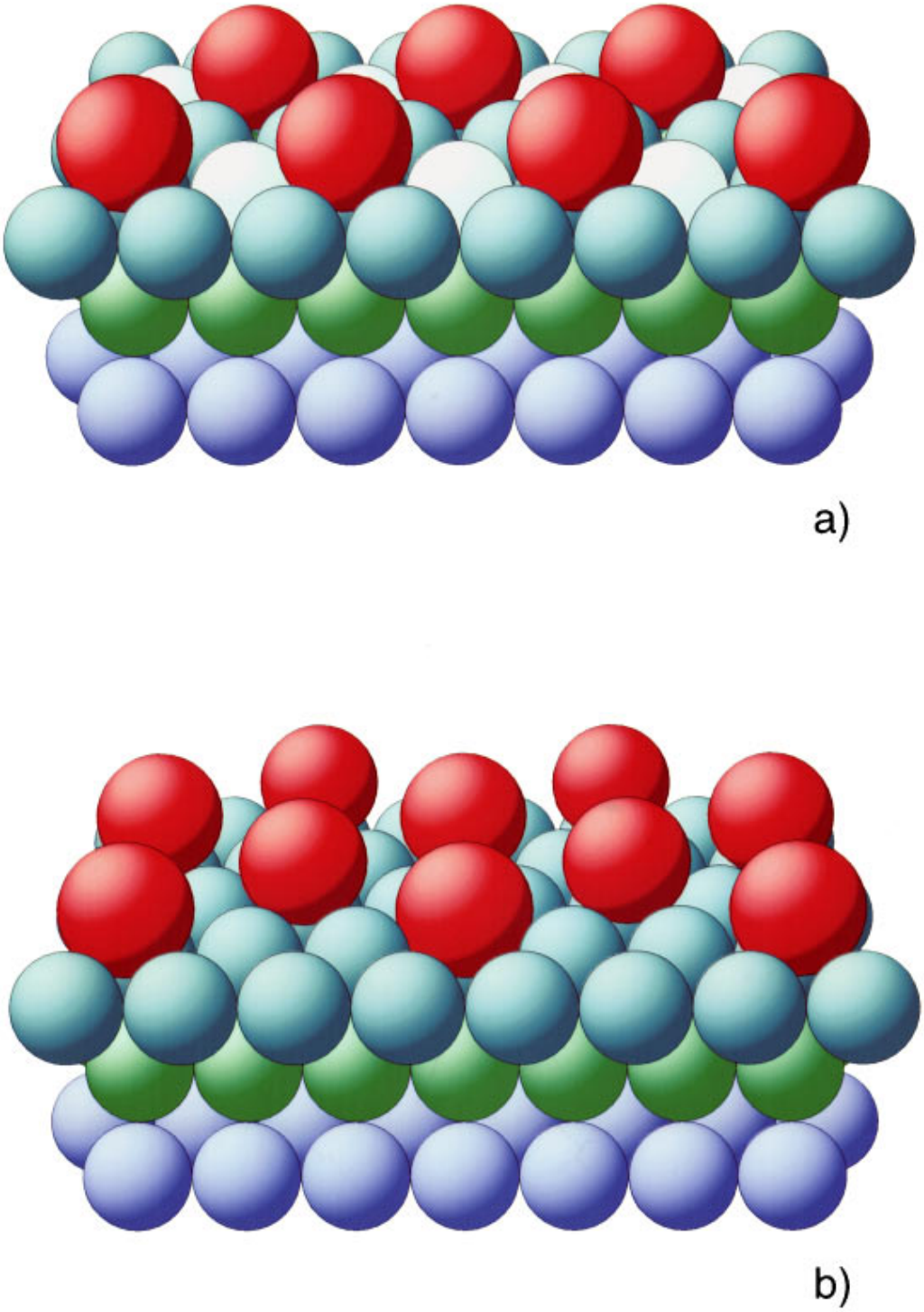

FIG. 5. (Color) (a) Perspective view of the best-fit structure model for the Pt{111}(2 × 2)-K structure. Smaller circles (gray, green, and blue) represent Pt atoms; large red circles correspond to K atoms. Lighter circles in the first Pt layer indicate Pt atoms displaced by 0.07 Å towards the bulk. (b) Perspective view of the best-fit structure model for the Pt{111}($\sqrt{3}\times\sqrt{3}$)$R30°$-K structure. Small circles represent Pt atoms, large darker circles correspond to K atoms.

and Bertel also suggest a return to on-surface adsorption at about $\Theta = 0.25$. Substitutional adsorption sites will be discussed in more detail in Sec. VI F.

C. Split positions analysis of in-plane K vibrations

Surface vibrations are usually accounted for in LEED analysis by a variation of the surface Debye temperature (and to a lesser extent by adjusting the imaginary part of the inner potential). The Debye temperature T_D, however, only accounts for isotropic vibrations, whereas adatoms on surfaces vibrate anisotropically. Additionally, it is possible to determine the anisotropic vibrational amplitudes with the split position approach:[14] The vibrating K atom is replaced by three equivalent atoms of weight 1/3, each laterally displaced

TABLE I. R_P factors for the different phases of Pt{111}-K studied. Numbers in brackets are calculated using the ''split positions'' analysis.

	hcp	fcc	Bridge	Atop	Fig. 3(e)	Fig. 3(f)
(2×2)						
$R_P^{\text{off-normal}}$	0.40 (0.35)	0.61	0.60	0.69	0.57	0.58
R_P^{normal}	0.38 (0.29)	0.81	0.54	0.60	0.44	0.47
$(\sqrt{3}\times\sqrt{3})R30°$						
$R_P^{\text{off-normal}}$	0.32 (0.22)	0.73	0.59	0.64	0.87	0.69
R_P^{normal}	0.29 (0.24)	0.68	0.71	0.82	0.68	0.61

by r_{split} from the mean position. Multiple scattering between these split atoms is suppressed and the Debye temperature is refined along with the split positions. The split positions method increases the apparent Debye temperature because it already accounts for part of the vibrations parallel to the surface. (A high Debye temperature correlates with small vibrational amplitudes.) The use of split positions reduces R_P by about 25% (see Table I). The calculated in- and out-of-plane vibrational amplitudes δr_{vib} and the isotropic Debye temperatures T_D are listed in Table II. These values are similar to those values found for K on Rh{111} (Ref. 18) and also compare reasonably well with the calculated values in Sec. VI C.

V. TOTAL-ENERGY CALCULATIONS

The first-principles total-energy calculations of clean and K-covered Pt{111} surfaces were performed using ''QUEST,'' a parallel code based on the linear combination of atomic orbitals (LCAO) method. A basis set of contracted Gaussians was used.[19] In the surface region several layers of floating orbitals were employed to make the basis set as complete as possible. The Ceperley-Alder LDA (Ref. 20) was applied to approximate the exchange-correlation (XC) interaction of the electrons. Hamann pseudopotentials[21] were used to represent the Pt and K cores. The theoretical lattice constant used was 3.895 Å , which is about 0.6% smaller than the experimental lattice constant in agreement with earlier calculations.[22,23] The Pt{111} surface was modeled by slabs seven or nine layers thick. The K adlayers plus the top two layers on each side of the slab were relaxed until all forces were below 10^{-2} eV/Å. To calculate the $(\sqrt{3}\times\sqrt{3})R30°$ and (2×2) adsorbate phases slabs with three to six Pt atoms per layer in hexagonal or orthorhombic supercells were used. The equivalent of up to 28 points were sampled in the irreducible portion of the surface Brillouin zone of a (1×1) unit cell. Tests with different cells, different k meshes, and different sets of floating orbitals indicated that calculated adsorption energy differences are accurate to within a few hundredths of an eV. The difference between fcc and hcp adsorption sites changed by a few meV only when different k meshes were used.

A. bcc K and KCl

Special care was necessary in the present work to generate transferable K pseudopotentials. For example, the calculated lattice constant of KCl is more than 20% too small if ''standard'' settings for the K pseudopotential are used. To get acceptable agreement with the experimental bulk properties of bcc K and KCl we used a highly ionic K atomic reference ($K^{+0.9}$). To describe the d channel scattering of the K correctly the r_c radius for the d pseudo-wave-function has to be small (0.79 Å). The evaluation of the valence-core XC interaction requires the use of a pseudocore charge (r_c=1.4 Å).[24] Using this recipe the calculated lattice constants of bcc K and of KCl were found to be about 3% below the experimental value. The bulk modulus is overestimated by about 50% in both cases. The disagreement between LDA calculations and experiment is slightly larger than usual. In the case of bcc K the inclusion of zero-point vibrations should improve the theoretical values, for KCl the use of the frozen core approximation might be the major source of error. For the purpose of this paper, however, it is most impor-

TABLE II. Structural parameters of the best fit model, i.e., the hcp site, from the LEED analysis together with the geometry parameters from the LDA calculations. LDA results are scaled to correct for the 1% underestimation of the Pt bulk lattice constant. Values given in percent relate to the bulk interlayer spacing.

	(2×2)		$(\sqrt{3}\times\sqrt{3})R30°$	
	LEED	LDA	LEED	LDA
K-Pt bond length (Å)	3.12±0.04	3.11	3.15±0.02	3.14
K-Pt layer separation (Å)	2.70±0.03	2.63	2.71±0.02	2.69
first Pt layer expansion Δd_{12} (%)	1.0±1.0	1.0	1.0s±0.02	1.0
second Pt layer expansion Δd_{23} (%)	0.0±1.0	0.0	-0.5±0.03	-0.6
first layer rumpling D_{11} (Å)	0.07±0.02	0.07		
$\delta r_{\text{vib}}^{\text{normal}}$(Å)	0.1±0.05		0.08±0.05	0.05
$\delta r_{\text{vib}}^{\text{parallel}}$(Å)	0.47±0.25		0.26±0.1	
Pottassium T_D (K)	250±70		200±30	
Platinum T_D (K)	302±50		302±50	

tant that the K/Pt interaction is described correctly. The good agreement between theory and the LEED experiment for the geometry of K adsorbed on Pt{111} indicates that the description of the K atom is quantitatively correct.

VI. LDA ENERGETICS, GEOMETRIES, AND ELECTRONIC STRUCTURE

A. Clean Pt{111}

Clean Pt{111} has previously been studied both theoretically[22,23] and experimentally.[15] The calculations reported here are in agreement with these earlier results in that the first interlayer spacing is expanded by 0.5% and the second-layer spacing is contracted by 0.6%. However, the calculated first-layer expansion is slightly smaller than the LEED result ($\Delta d_{12} \simeq 1\%$ according to Ref. 15 and this work). Also, the LEED analysis does not predict any significant second-layer expansion. A slight disagreement between LDA and LEED analysis for clean transition-metal surfaces seems to be unavoidable.[25] We note, however, that theory and experiment agree on a slight first-layer expansion. Like the fcc/hcp difference discussed in Sec. VI E, the expansion is caused by a polarization of surface *d* electrons.

B. Geometry of the K-covered Pt{111} surface from LDA

For both coverages studied the K adatom prefers the hcp site over the fcc site with a geometry that is close to the LEED result. Other adsorption sites on the flat surface were not studied. In the following comparison we account for the underestimation of bond lengths in LDA by scaling the calculated distances by a factor 1.01. In the $(\sqrt{3}\times\sqrt{3})R30°$ structure the K atoms are separated from their Pt neighbors by 3.14 Å. The K adlayer to Pt top layer distance is 2.69 Å. Both numbers are within 1% of the LEED result. The first Pt layer expansion is 1.0% and the second is -0.6%, both practically identical with the LEED $I(V)$ analysis above. Complementary to the LEED analysis, which is not sensitive to very small shifts parallel to the surface, we have also allowed for an in-plane relaxation of the top two Pt layers. A 0.8% in-plane expansion of the triangle of Pt atoms beneath the K adsorbate was found. In the (2×2) phase the Pt-K distance is reduced by 1% to 3.11 Å relative to the $(\sqrt{3}\times\sqrt{3})R30°$ phase, again confirming the results of the LEED analysis. This indicates a smaller radius and larger ionicity of the K adatom, which correlates with the fact that the measured work-function minimum is near a K coverage of $\Theta = 0.25$.[26] The height of the K adlayer above the average Pt surface atom is 2.63 Å. The surface Pt atoms that are not nearest neighbors of the K adatoms are raised relative to the other Pt surface atoms by 0.07 Å (D_{11}). The in-plane expansion of the triangle of Pt atoms beneath the K is 0.9%.

C. K vibrations normal to the surface at a coverage of $\Theta = 0.33$

To support the identification of the hcp hollow as the adsorption site the frequency of the perpendicular K vibration at Γ for the $(\sqrt{3}\times\sqrt{3})R30°$ structure was determined. A vibrational frequency of 154 cm^{-1} was obtained by fitting the total energy and the forces on the K for four vertical displacements z of the K adlayer to a third-order polynomial $E(z)$. The Pt substrate was held fixed in these calculations. This result is in almost perfect agreement with EELS measurements (152 cm^{-1}) by Hannon *et al.*[27] for the $(\sqrt{3}\times\sqrt{3})R30°$ phase; the very good agreement indicates that the K-Pt and the Pt-Pt vibrations are only weakly coupled. This is confirmed by the observation of only a very small width of the K-induced EELS peak at 152 cm^{-1} in the experiment.[27] The calculated mean vibrational amplitude $\delta r_{\mathrm{vib}}^{\mathrm{normal}}$ is 0.05 Å at a temperature of 100 K, assuming an energy of $1/2kT$ in the vibration normal to the surface (see Table II). This is within the error margin of the value derived from the split position LEED analysis (0.08 ± 0.05).

D. Coverage dependence of the dipole moment and the adsorption energy

At low coverages alkali-metal adsorbates usually repel each other, whereas in the high coverage limit some alkali films actually condense.[28,17] We have found no condensation for K adsorbed on P{111}. K adatoms repel each other up to the saturation coverage of $\Theta = 0.33$ according to our LDA calculations. At this coverage the adsorption energy is 2.42 eV; at $\Theta = 0.25$ the value is 2.93 eV. K-K repulsion at all coverages is also indicated by the structural phase diagram for K adlayers on Pt{111} in which all observed phases minimize the K-K dipole-dipole repulsion.[4] The dipole moment per K adatom can be determined from the calculated K-induced work-function change: The work function is reduced from 6.1 eV for clean Pt{111} to 1.2 eV at $\Theta = 0.25$. At $\Theta = 0.33$ partial depolarization leads to a work function of 1.7 eV. The work-function reductions of 4.9 eV at $\Theta = 0.25$ and 4.4 eV at $\Theta = 0.33$ result from dipole moments per K adsorbate of 3.4 D and 2.3 D, respectively.[29] The calculated work function changes are in reasonable agreement with measured values of 4.4 eV and 4.1 eV.[26] Comparison with experiment also shows that the depolarization with coverage is quite substantial. In the zero coverage limit the measured dipole moment per K adatom is 9.4 D.[26]

Besides the dipole-dipole repulsion an additional contribution has to be taken into account. At $\Theta = 0.33$ coverage the K-K distance is only 4% larger than the K bcc nearest-neighbor distance and a direct K-K bonding interaction starts to occur. The K-K interaction reduces the strength of the K-Pt bonds although they remain much stronger: The K bulk cohesive energy is 0.9 eV and the K adsorption energy on Pt{111} is almost 3 eV at low coverage.[2] This does not induce a condensed phase, but does give rise to the 0.51 eV difference in adsorption energy between $\Theta = 0.25$ and $\Theta = 0.33$. It is thus unfavorable to weaken the K-Pt bond in favor of a metallic K-K bond. This relatively strong K-Pt bond is a major difference found when comparing the present system with K adsorption on Al{111}.[28] The adsorption energy of K on Al(111) at high coverage is only 40% higher than the K bulk cohesive energy[28] thus allowing an attractive K-K interaction. Between $\Theta = 0.25$ and $\Theta = 0.33$ the K adsorption energy on Al{111} increases slightly.[28] It is remarkable that the condensed K adlayer phase forms on Al{111} at $\Theta = 0.33$ even though the K-K distance is still 7.6% larger than the bulk K-K distance, indicating that the

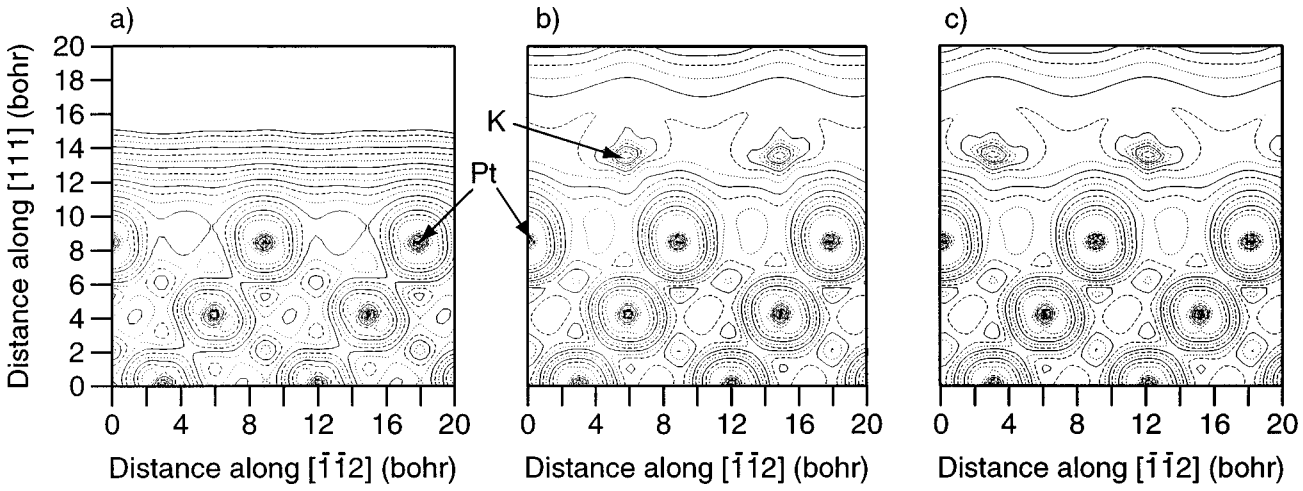

FIG. 6. (a) Calculated valence charge density in a normal cut through the clean Pt{111} surface. (b) Cut through local density of states of K on Pt{111} at threefold hcp sites for $\Theta = 0.33$. The contributing states are 1 ± 1 eV below the Fermi energy. (c) Same as (b) but with K in the fcc hollow site.

K-K interaction should be substantial in the $(\sqrt{3} \times \sqrt{3})R30°$ phase on Pt{111} as assumed above.

E. The origin of the hcp-fcc site energy difference

The hcp site is preferred over the fcc site by about 15 meV for both coverages studied here. Even in the zero coverage limit the hcp site is preferred for K on Pt{111} according to Müller's cluster calculations.[5,6] A calculated energy difference of 15 meV is quite small considering the approximations involved in the calculations and we would rather be more careful were it not for the LEED results. The preference for the hcp site can actually be traced back to differences in the electronic structure at the fcc and the hcp sites. Pt has an outer *d* shell that is almost full. The *d* electrons just below the Fermi energy thus have antibonding character. At the surface the in-plane *d* charge is reduced and the *d* orbitals with mostly out-of-plane character get filled instead [see Fig. 6(a)], thus keeping the top Pt layer approximately charge neutral. This intra-atomic charge reorganization reduces the in-plane *d* repulsion and adds to the repulsion between the first and second layers. This lowers the energy because the surface layer has only neighbors towards the bulk. The *d* charge reorganization contributes to the surface expansion (see Sec. VI A) and to the large in-plane tensile surface stress of Pt{111}.[30,23]

That the *d* states just below the Fermi energy contribute repulsively to the Pt-Pt interaction can be seen in Fig. 6(a). The *d* contours for the surface layer are slightly tilted to the left, i.e., towards the hcp site, so that the *d* hole points partially to the Pt neighbors in the the second layer. If the *d* states just below the Fermi energy contributed attractively to the Pt-Pt interaction the *d* charge in Fig. 6(a) would tilt to the right. Figures 6(b) and 6(c) show the density of states approximately 1 eV below the Fermi energy with K adsorbed on the hcp and the fcc sites, respectively. The K adlayer enhances the vertical polarization of the Pt surface atoms *d* states, indicating an attractive electrostatic interaction between the Pt *d* electrons and the positively charged K adlayer. The extra vertical polarization also adds to the surface expansion, at least in the LDA calculations. As discussed above, the *d* charge tilts towards the hcp site and leads to an extra attraction of the K adatom towards the hcp site.

This electrostatic model describing the preference of K for the hcp site is related to Feibelman's model for oxygen adsorption on Pt{111}.[32] O prefers the fcc site over the hcp site by about 0.5 eV on this surface. The negatively charged O adatoms repel the *d* shell of the surface atoms, which causes the neighboring Pt *d* hole to orient away from the O. This is favorable for the O on the fcc site, but leads to extra Pt-Pt repulsion on the hcp site.[32]

The *d* polarization model is also consistent with alkali-metal adsorption on Rh{111} and Ru{0001}, which has been studied earlier with dynamical LEED analysis.[14,18] In the case of Rh{111}, which has about eight *d* electrons, the highest occupied *d* orbital should still be antibonding in nature so that a preference of alkali metals for the hcp site is expected. In hcp Ru it is not clear whether the highest occupied *d* orbitals — Ru has two *d* electrons less than Pt — are bonding, nonbonding, or anti-bonding.[31] The energy difference between the fcc and hcp sites should be relatively small. This is in agreement with the experiment, which shows the fcc site occupied at a coverage of $\Theta = 0.25$.[18]

Our model for the fcc-hcp difference only considers the interaction of the *d* electrons with the alkali-metal adsorbate; the *s-p* electrons are neglected. This seems justified because metals where the *d* electrons do not contribute significantly to the bonding show an even smaller fcc-hcp site difference for alkali-metal adsorption. For example, on Ag{111} both fcc and hcp sites have been found,[17] and on Al{111} the calculated fcc-hcp energy difference is only about 1 meV for Na or K adsorption according to our calculations (see also Ref. 28).

F. Energies for substitutional adsorption

Two recent papers indicate a possible substitutional adsorption site for K on Pt{111}.[7,6] This seems unlikely because it would mean that it is favorable for Pt-Pt bonds to be replaced by Pt-K bonds: in fact the Pt cohesive energy is six times larger than that of bcc K and still double the adsorption energy of K on Pt{111}. Not surprisingly, the cluster calcu-

lations of Müller[6] indicate that K adsorption in single ($\Delta E = 0.6$ eV) or triple ($\Delta E = 0.9$ eV) surface vacancies is unfavorable at low K coverage. Also the subsurface vacancy site is unfavorable by 1.15 eV compared to on-surface adsorption. It is argued in Ref. 6 that the substitutional geometries become favorable at higher coverage because of the K-K repulsion on the flat surface.

To test whether K substitutional adsorption might be of lower energy on flat Pt{111} at high K coverage we first considered a $(\sqrt{3}\times\sqrt{3})R30°$ arrangement of K-filled surface vacancies [Fig. 3(e)]. This is the lowest-energy phase for high coverages of Na and K on Al{111}.[13,28] K in a surface vacancy on Pt{111} would be a first step in the process of subsurface adsorption. Our calculations show that it costs 0.48 eV per K atom to form the vacancy structure instead of the on-surface phase at $\Theta = 0.33$. The energy difference of 0.48 eV is the result of a Pt{111} surface vacancy formation energy in a $(\sqrt{3}\times\sqrt{3})R30°$ arrangement with the displaced Pt atom put in a bulk site of 1.49 eV (Ref. 33) and a 3.43 eV binding energy of the K atom in the vacancy. Thus the K is 1.01 eV more stable in the vacancy than on the flat surface at $\Theta = 0.33$ coverage. This is not enough, however, to compensate for the Pt{111} surface vacancy.

We have also considered a second geometry where Pt-Pt bonds are broken in favor of K-Pt bonds: a 1/4 ML of Pt adatoms on the fcc site embedded in a K adlayer on hcp sites at $\Theta = 0.25$. This geometry is less favorable by 1.26 eV per K atom compared to a surface K adlayer at $\Theta = 0.25$ K and the Pt adatoms remaining the bulk. Again, the K atoms are bound more strongly at the more open surface. The K-Pt binding energy increases from 2.93 to 3.35 eV. This is caused by a doubling of the number of Pt neighbors and a better screening of the K from each other. However, this energy gain is too small to compensate for the Pt adatom formation energy of 1.68 eV that we calculate. Our calculations provide additional insight as to the cost in energy required to form a K substitutional structure on flat Pt{111}. Combining the surface adatom and the surface vacancy formation energies on Pt{111} at high K coverage (0.48 eV) we obtain an estimate of the formation energy for the Pt surface Frenkel pair on K-covered Pt{111} of 0.48 + 1.26 = 1.74 eV. This energy is an approximate lower limit for the barrier to incorporate K on flat Pt{111}.

To test if subsurface K adsorption is favorable, we have investigated K embedded in the second layer of a Pt{111} slab and replacing one or three Pt atoms. A (2×2) cell was used for these calculations and the K plus the top three Pt layers of a Pt{111} slab were allowed to relax. It turns out that both geometries are very unfavorable. Again a bulk reservoir for the removed Pt atoms is assumed. The resulting K adsorption energies are below 0.5 eV. One reason for the high energy of subsurface K is that the vacancy formation energy in bulk Pt should be almost twice the surface value.[33] The other reason is that the K substitutional atom does not fit well into the Pt bulk matrix. For example, in the single vacancy the K is too large and leads to an expansion of the first-layer spacing of 8% and of the second of 4%. If the K replaces two or three Pt atoms the space available for the K is not spherical enough.

Interstitial K absorption has not been calculated. We assume that because of the size of the K atom interstitial absorption of K in Pt is even less likely than substitutional adsorption.

Although they cannot be described as an exhaustive study of all possible substitutional geometries of K on Pt{111}, the LDA calculations by Müller and those presented here together show that it is generally unfavorable to replace Pt-Pt bonds by K-Pt bonds even at high K coverage. This conclusion is supported by the present LEED study, which excludes the two possible substitutional adsorption geometries (Figs. 3(e) and 3(f) as well as Table I). Nevertheless, substitutional K adsorption might still take place at vacancies at steps. This could explain the ''fuzziness'' of the steps in the STM images of K-covered Pt{111}.[6] Energetic reasons favor incorporation at steps: Vacancy formation energies are much smaller at steps than on flat (111) surfaces because fewer bonds have to be broken. The vacancy formation energy at a step on Al{111} is about 1/3 of that on flat Al{111}.[34] Already a reduction by 50% would be enough to make substitutional K at steps on Pt{111} stable.[35]

VII. CONCLUSIONS

K adsorbs in the hcp hollow site in both the (2×2) and the $(\sqrt{3}\times\sqrt{3})R30°$ phases of K on Pt{111}. The properties of the K adlayer are similar to those predicted by the Gurney model. The energy difference between the hcp site and the fcc site is quite small (15 meV), but significant; it results from the antibonding nature of the highest occupied Pt *d* states. These are strongly polarized at the Pt{111} surface.

The geometrical parameters for the two phases determined independently with LEED structure analysis and LDA calculations agree quite well. Moreover, the frequencies of the K vibration of all modes determined with LEED, LDA, and EELS (Ref. 6) are consistent.

On the basis of LDA total-energy calculations of substitutional K adsorption energies and an analysis of the relative bond strength of Pt-Pt and Pt-K bonds we can exclude the possibility that a large fraction of a K monolayer adsorbs substitutionally in surface or subsurface. The most likely candidates for substitutional adsorption sites are vacancies at steps. However, without measurement or calculation we can already predict that the vibrational frequencies of K at vacancies at steps will be lower than the 225 cm^{-1} considered to be the signature of the subsurface K in Ref. 6. The puzzle concerning the possible substitutional adsorption of K on Pt{111} is not yet solved.

ACKNOWLEDGMENTS

We are indebted to W. Moritz for supplying the platinum phase shifts and to J.B. Hannon, P. J. Feibelman, M. Gierer, and H. Over for valuable discussions. This work has been supported both by the Deutsche Forschungsgemeinschaft within the Sonderforschungsbereich 290 and by the United States Department of Energy under Contract No. DE-AC04-94AL85000. Sandia is a multiprogram laboratory operated by Sandia Corporation, a Lockheed Martin Company, for the United States Department of Energy.

[1] G. Pirug and H.P. Bonzel, Surf. Sci. **122**, 1 (1982).
[2] E.L. Garfunkel and G.P. Somorjai, Surf. Sci. **115**, 441 (1982).
[3] G. Pirug and N. P. Bonzel *et al.*, Surf. Sci. **194**, 159 (1988).
[4] H. Arce, W.L. Mochan, and J.J. Gutierez, Surf. Sci. **348**, 379 (1996).
[5] J.E. Müller in *Physics and Chemistry of Alkali Metal Adsorption*, edited by H.P. Bonzel, A.M. Bradshaw, and G. Ertl (Elsevier, Amsterdam, 1989), p. 271.
[6] J.B. Hannon, M. Giesen, C. Klünker, G. Schulze Icking-Konert, D. Stapel, and H. Ibach, Phys. Rev. Lett. **78**, 1094 (1997).
[7] J. Lehmann, P. Ross, and E. Bertel, Phys. Rev. B **54**, 2347 (1996).
[8] W. Moritz, J. Phys. C **17**, 353 (1988).
[9] J.B. Pendry, *Low Energy Electron Diffraction* (Academic, London, 1974).
[10] V.L. Moruzzi, J.F. Janak, and A.R.Williams, *Calculation of Electronic Properties of Metals* (Plenum, New York, 1978).
[11] J.B. Pendry, J. Phys. C **13**, 937 (1980).
[12] G. Kleinle, W. Moritz, and G. Ertl, Surf. Sci. **238**, 119 (1990).
[13] A. Schmalz *et al.*, Phys. Rev. Lett. **67**, 2163 (1991); J. Neugebauer and M. Scheffler, Phys. Rev. B **46**, 16 067 (1992).
[14] S. Schwegmann and H. Over, Surf. Sci. **360**, 271 (1996).
[15] N. Materer, U. Starke, A. Barbieri, R. Döll, K. Heinz, M.A. van Hove, and G.P. Somorjai, Surf. Sci. **325**, 207 (1995); K. Hajeck, H. Glassl, A. Guttmann, and H. Leonard, *ibid.* **152**, 419 (1985); D.L. Adams, H.B. Nielsen, and M.A. Van Hove, Phys. Rev. B **20**, 4789 (1979).
[16] G.M. Lamble, Ph.D. thesis, The University of Liverpool, 1986.
[17] R.D. Diehl and R. Mc. Grath, Surf. Sci. Rep. **23**, 138 (1996).
[18] H. Over, M. Gierer, H. Bludau, and G. Ertl, Phys. Rev. B **52**, 16 812 (1995).
[19] The Pt basis set is that used in Refs. 22,23. The Pt and the K two *s*-, two *d*-, and one *p*-like radial functions are used. Additionally, four to five floating *s*-like orbitals per Pt surface atom are added to improve the description of the charge falloff at the surface-vacuum interface. The position of those orbitals is fully relaxed.
[20] D.M. Ceperley and B.J. Alder, Phys. Rev. Lett. **45**, 566 (1980) as parametrized by J.P. Perdew and A. Zunger, Phys. Rev. B **23**, 5048 (1981).
[21] D.R. Hamann, Phys. Rev. B **40**, 2980 (1989).
[22] P.J. Feibelman, Phys. Rev. B **52**, 16 845 (1995).
[23] P.J. Feibelman, Phys. Rev. B **51**, 17 867 (1995).
[24] S.G. Louie, S. Froyen, and M.L. Cohen, Phys. Rev. B **26**, 1738 (1982).
[25] P.J. Feibelman, Surf. Sci. **360**, 297 (1996).
[26] M. Kiskinova, G. Pirug, and H.P. Bonzel, Surf. Sci. **133**, 312 (1983).
[27] J.B. Hannon (private communication).
[28] J. Neugebauer and M. Scheffler, Phys. Rev. Lett. **71**, 577 (1993).
[29] Work-function change $\delta\phi$ and dipole moment μ of an adsorbate are related by the Helmholtz equation $\delta\phi = -2\pi\mu n_a$ with an
[30] R.J. Needs and M. Mansfield, J. Phys.: Condens. Matter **1**, 7555 (1989).
[31] P.J. Feibelman, S. Esch, and T. Michely, Phys. Rev. Lett. **77**, 2257 (1996); P.J. Feibelman (unpublished).
[32] In the case of O adsorption on Ru(0001) Feibelman argues that the nature of the highest occupied *d* orbitals is nonbonding (unpublished).
[33] Our calculated vacancy formation energy of 1.49 eV is similar to that calculated for Rh{111}, 1.32 eV, in the same $(\sqrt{3}\times\sqrt{3})R30°$ arrangement by H. M. Polatoglou, M. Methfessel, and M. Scheffler, Phys. Rev. B **48**, 1877 (1993). Rh and Pt should have similar vacancy formation energies because their cohesive energies are comparable (5.84 eV for Pt and 5.75 eV for Rh). Polatoglou *et al.* also calculate the Rh bulk vacancy formation energy, which is 2.26 eV and should be a good estimate for Pt.
[34] R. Stumpf and M. Scheffler, Phys. Rev. B **53**, 4958 (1996).
[35] In the case of substitutional adsorption of Na on Al{111} it has been found that Na adatoms prefer vacancies at steps to vacancies on flat Al{111} by about 0.5 eV. This difference includes the vacancy formation energy difference. Thus it is not surprising that the $(\sqrt{3}\times\sqrt{3})R30°$ vacancy reconstruction starts to form at steps according to H. Brune, J. Wintterlin, R.J. Behm, and G. Ertl, Phys. Rev. B **51**, 13 592 (1995).